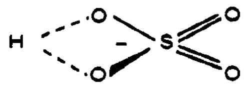

A

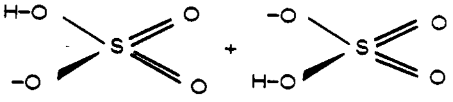

B

distances) have substantially larger thermal vibration ellipsoids than do O(6) and O(7). Unfortunately, we have no simple explanation for these two perturbations; a purely librational shortening of S(1)-O(4) and S(1)-O(5) is unlikely.

Summary

The observed reaction shows the ready displacement by carbon monoxide of ligands bound through oxygen to the Ir(III) center.

$$\mathrm{Ir(CO)(OH)(SO_4)L_2} + 3\mathrm{CO} \rightarrow [\mathrm{Ir(CO)_3L_2}^+][\mathrm{HSO_4}^-] + \mathrm{CO_2} \quad (8)$$

$$\mathrm{L} = \mathrm{PPh_3} \text{ or } \mathrm{P}(p\text{-tolyl})_3$$

The formation of CO_2 almost certainly occurs by displacement of the hydroxide by CO, followed by attack of the OH^- on the carbon of a carbonyl of the cationic complex to form an iridium carboxylic acid.[20,31] Such complexes are known to eliminate CO_2.[31] The sequence to $Ir(CO)(OH)(SO_4)L_2$, L = PPh_3 or $P(p\text{-tolyl})_3$, and its subsequent reaction with CO leads from Ir(I) and back to Ir(I) and can be presented as

$$\mathrm{OH}^- + \mathrm{O_2} + \mathrm{SO_2} + \mathrm{CO} \xrightarrow{\mathrm{Ir(I)}} \mathrm{HSO_4}^- + \mathrm{CO_2} \quad (9)$$

This reaction, which has considerable environmental importance, is not completely accurate because the Ir(I) is not a catalyst in the currently described reaction. However, it provides a useful example of the potential for unusual transformations on transition-metal centers containing mixtures of hard and soft ligands.

Reaction 8 provides the third example[20,28] of displacement by CO of ligands coordinated through one or more oxygen atoms to iridium(I) or iridium(III) at ambient conditions. Thus, "hard" ligands that are bound to relatively soft metal centers exhibit considerable lability.

Acknowledgment. We acknowledge support from the National Science Foundation (Grant CHE-8709563) and a loan of $IrCl_3{\cdot}3H_2O$ by Johnson Matthey, Inc.

Supplementary Material Available: Tables of anisotropic displacement coefficients and H atom coordinates (3 pages); a listing of observed and calculated structure factor amplitudes (18 pages). Ordering information is given on any current masthead page.

---

[31] Bennett, M. A.; Robertson, G. B.; Rokicki, A.; Wickramasinghe, W. A. *J. Am. Chem. Soc.* 1988, *110*, 7098.

Ferromagnetic Behavior of Linear-Chain Electron-Transfer Complexes. Synthesis and Characterization of Decaethylferrocene, $Fe(C_5Et_5)_2$, and Its Electron-Transfer Salts: Structure and Magnetic Properties of $[Fe(C_5Et_5)_2]^{\bullet+}[A]^{\bullet-}$ [A = TCNE and TCNQ]

Kai-Ming Chi,[1a,b] Joseph C. Calabrese,[1a] William M. Reiff,*,[1c] and Joel S. Miller*,[1a]

Central Research and Development Department, E. I. du Pont de Nemours and Company, Experimental Station E328, Wilmington, Delaware 19880-0328, Department of Physics, The Ohio State University, Columbus, Ohio 43210-1106, and Department of Chemistry, Northeastern University, Boston, Massachusetts 02115

Received July 31, 1990

1,2,3,4,5-Pentaethylcyclopentadiene as well as $Fe(C_5Et_5)_2$ (D) and several electron-transfer salts have been prepared. The structure of the $[TCNQ]^{\bullet-}$ (A) salt has been determined [A = 9.416 (2) Å, b = 9.966 (1) Å, c = 11.710 Å, α = 93.83 (1)°, β = 109.29 (1)°, γ = 109.05 (1)°, V = 961.4 Å^3, Z = 1, T = -70 °C] to have a $\cdots D^{\bullet+}A^{\bullet-}D^{\bullet+}A^{\bullet-}\cdots$ structural motif. The ^{57}Fe Mössbauer spectra of $[TCNE]^{\bullet-}$ and $[TCNQ]^{\bullet-}$ salts of $[Fe(C_5Et_5)_2]^{\bullet+}$ are typical of ferrocenium ions and magnetic hyperfine splitting characteristic of either slow paramagnetic relaxation or extended magnetic order is not observed above 1.5 K. The 5-K EPR spectrum of $[Fe(C_5Et_5)_2]^{\bullet+}$ has a strong absorption at $g_\parallel$ = 4.59. The Faraday magnetic susceptibility (2-320 K) can be fit to the Curie-Weiss expression, μ_{eff} = 3.37, 3.15, and 3.62 μ_B and θ = 6.9, 7.5, and 6.1 K, for the $[PF_6]^-$, $[TCNE]^{\bullet-}$, and $[TCNQ]^{\bullet-}$ salts of $[Fe(C_5Et_5)_2]^{\bullet+}$, consistent with ferromagnetic coupling, respectively.

Introduction

Pentamethylcyclopentadienyl, C_5Me_5, Cp*, has been widely used as an electron-donating ligand in organometallic chemistry, and convenient synthetic routes to C_5Me_5H have been reported.[2] The synthesis of the ethyl analogue, 1,2,3,4,5-pentaethylcyclopentadiene (1), however, has not been reported. With the observation of bulk ferromagnetic behavior for the electron-transfer salt of decamethylferrocene, $FeCp^*_2$, and tetracyanoethylene,

---

[1] (a) Du Pont. (b) Ohio State University. (c) Northeastern University.

[2] Baker, R. T. *Inorg. React. Methods*, in press. Maitlis, P. *Chem. Soc. Rev.* 1981, *10*, 1. King, R. B.; Bisnette, M. B. *J. Organomet. Chem.* 1967, *8*, 287.

0276-7333/91/2310-0688$02.50/0 © 1991 American Chemical Society

TCNE,[3,4] and metamagnetism for the electron-transfer salt of $FeCp^*_2$ and 7,7,8,8-tetracyano-*p*-quinodimethane, TCNQ,[3,5] we sought to prepare the $Fe(C_5Et_5)_2$ electron-transfer salt with TCNE and TCNQ and ascertain if they exhibit cooperative magnetic properties.

Experimental Section

2,3,4,5-Tetraethylcyclopent-2-enone (2). A 500-mL three-necked flask equipped with condenser, septum, and N_2 gas inlet was charged with 32.8 g (0.4 mol) of 3-hexyne, 200 mL of EtOH, and 40 mL of concentrated HCl. The solution was cooled to -40 °C and $Ni(CO)_4$ (89 g, 0.52 mol) was added by syringe. The solution was stirred and slowly warmed to room temperature before it was heated at 60 °C for 6 h and gradually turned green. After cooling to room temperature, water (150 mL) was added. The organic layer was separated, and the aqueous layer was extracted with ether (2 × 50 mL). After the organic phases were combined and dried with $MgSO_4$, the solvent was removed with a rotary evaporator. Distillation of the remaining liquid under reduced pressure (ca. 10 mm) provided a colorless liquid (7.8 g) at 48–50 °C and a pale yellow liquid (19.6 g) at 85–87 °C. The ^1H NMR spectra showed that the former was the ester **3** and the latter was **2**. When this reaction is carried out in acetone instead of ethanol, the side product is the corresponding acid of **3**, which has a boiling point close to that of **2** and was difficult to isolate.

Preparation of 1. A solution of 3.0 M EtMgBr (30 mL, 90 mmol) in Et_2O was added to a 500-mL flask containing **2** (16 g, 82 mmol) in 100 mL of Et_2O at -40 °C. The solution was stirred and warmed to room temperature, and a white precipitate formed. Sitring was continued for an additional 5 h, and then a dilute solution of HCl (25 mL) was added. After 3 h of stirring the organic layer was separated and dried with $MgSO_4$. The solvent was distilled at atmospheric pressure and a colorless liquid product (10.7 g) was collected by vacuum distillation (ca. 10 mm) at 55–57 °C. The ^1H NMR spectrum indicated that **1** and another species were present; however, attempts to separate them were unsuccessful.

$Li(C_5Et_5)$. An excess amount of *n*-BuLi solution in hexane was added to a solution of **1** in hexane. After stirring for 6 h, concentration of the solution provided white solids, which were collected and washed with a minimum of hexanes and vacuum-dried. About 5 g of $Li(C_5Et_5)$ was obtained, and its ^1H NMR spectrum showed two broad resonances at 1.03 and 2.39 ppm (intensity ratio is 3:2) in THF-d_8.

Bis(1,2,3,4,5-pentaethylcyclopentadienyl)iron, $Fe(C_5Et_5)_2$. A solution of $Li(C_5Et_5)$ (1.95 g, 9.18 mmol) in 50 mL of THF was added to $FeCl_2{\cdot}2THF$ (1.24 g, 4.58 mmol) in 100 mL of THF at 0 °C. The solution immediately became dark brown. After stirring for 3 h under N_2, the solution was exposed to air and stirred for an additional 2 h and the solution gradually turned yellow-brown. A brown powder was obtained after removal of the THF, and it dissolved in hexane to form a yellow solution. Filtration and removal of the hexane afforded a yellow sticky solid. Recrystallization from ether provided 1.0 g of yellow prisms $Fe(C_5Et_4)_2$ (48%). NMR ($CDCl_3$): ^1H 1.03 (t, 3 H, CH_3), 2.05 (br, 2 H, CH_2) ppm. $^{13}C\{^1H\}$ 86.5 (ring C), 18.2 (CH_2), 15.5 (CH_3) ppm. Anal. Calcd (found) for $C_{30}H_{50}Fe$: C, 77.23 (77.37); H, 10.80 (10.78).

$[Fe(C_5Et_5)_2]^{\bullet+}[TCNE]^{\bullet-}$. A solution of $Fe(C_5Et_5)_2$ (234 mg, 0.50 mmol) in 30 mL of THF was mixed with a solution of TCNE (Aldrich; 64 mg, 0.50 mmol) in 50 mL of THF, and the solution turned green. After stirring for 1 h, the solution was filtered and the THF was removed via rotary evaporator. The resulting solid was washed with hexane and vacuum dried. Recrystallization from THF by ether diffusion provided dark green needles (79%; 237 mg). Anal. Calcd (found) for $C_{36}H_{50}FeN_4$: C, 72.71 (72.56); H, 8.47 (8.20); N, 9.42 (9.89).

Table I. Crystallographic Details for $[Fe(C_5Et_5)_2][TCNQ]$

formula	$C_{42}H_{54}N_4Fe$
formula mass	670.77
space group	$P\bar{1}$ (No. 2)
a, Å	9.416 (2)
b, Å	9.966 (1)
c, Å	11.710 (2)
α, deg	93.83 (1)
β, deg	109.29 (1)
γ, deg	109.05 (1)
V, Å^3	961.4
Z	1
ρ(calc), g cm^{-3}	1.158
cryst dimens, mm	0.37 × 0.24 × 0.37
λ(radiation), Å	0.71073
abs coeff, cm^{-1}	4.22
T, °C	-70
$R(F_o^2)^a$	0.034
$R_w(F_o^2)^b$	0.041
scan mode	ω
2θ min, deg	4.9
2θ max, deg	60.0
scan width, deg ω	1.30–1.90
scan speed, deg	1.50–2.50
no. of total data measd	5835
no. of unique data with $F_o^2 > 3\sigma F_o^2$	4659
final no. of variables	322
weighting scheme	$\propto[\sigma^2(I) + 0.0009I^2]^{-1/2}$
largest residual, e Å^{-3}	0.31 near C(13)

$^a R = \sum[|F_o| - |F_c|]/\sum|F_o|$. $^b R_w = [\sum w[|F_o| - |F_c|]^2/\sum w|F_o|^2]^{1/2}$.

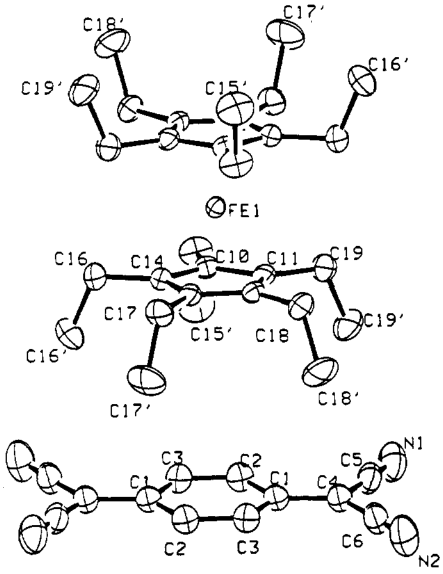

Figure 1. Atom labeling for $[Fe(C_5Et_5)_2]^{\bullet+}[TCNQ]^{\bullet-}$.

$[Fe(C_5Et_5)_2]^{\bullet+}[TCNQ]^{\bullet+}$ was prepared by the above method with TCNQ (Aldrich) (81%). Dark blue crystals were grown by ether diffusion into the THF solution. Anal. Calcd (found) for $C_{42}H_{54}FeN_4$: C, 75.21 (74.99); H, 8.11 (8.08); N, 8.35 (8.33).

$[Fe(C_5Et_5)_2]^{\bullet+}[PF_6]^-$. A solution of $Fe(C_5Et_5)_2$ (150 mg, 0.32 mmol) in 100 mL of THF was added to a solution of $[FeCp_2][PF_6]$ (90 mg, 0.27 mmol) in 50 mL of THF. The solution gradually turned from yellow to green during the 4 h it was stirred. Filtration and removal of the solvent gave a mixture of green and yellow solids. The $FeCp_2$ was removed via hexane extraction. After collection and vacuum-drying, 123 mg of $[Fe(C_5Et_5)_2][PF_6]$ was isolated (74%). Anal. Calcd (found) for $C_{30}H_{50}F_6FeP$: C, 58.92 (59.12); H, 8.24 (8.24).

$[Fe(C_5Et_5)_2]^{\bullet+}[BF_4]^-$ was prepared by the method outlined for $[FeCp^*_2]^{\bullet+}[BF_4]^-$ (92%).[4b] Anal. Calcd (found) for $C_{30}H_{50}BF_4Fe$: C, 65.11 (64.65); H, 9.11 (8.86).

---

(3) Miller, J. S.; Epstein, A. J.; Reiff, W. M. *Isr. J. Chem.* **1987**, *27*, 363. Miller, J. S.; Epstein, A. J.; Reiff, W. M. *Chem. Rev.* **1988**, *88*, 201. Miller, J. S.; Epstein, A. J.; Reiff, W. M. *Acc. Chem. Res.* **1988**, *21*, 114. Miller, J. S.; Epstein, A. J.; Reiff, W. M. *Science* **1988**, *240*, 40. Miller, J. S.; Epstein, A. J. *New Aspects of Organic Chemistry*; Yoshida, Z., Shiba, T., Ohsiro, Y. Eds.; VCH Publishers: New York, 1989; p 237.

(4) (a) Miller, J. S.; Calabrese, J. C.; Bigelow, R. W.; Epstein, A. J.; Zhang, J. H.; Reiff, W. M. *J. Chem. Soc., Chem. Commun.* **1986**, 1026. (b) Miller, J. S.; Calabrese, J. C.; Rommelmann, H.; Chittpieddi, S.; Zhang, J. H.; Reiff, W. M.; Epstein, A. J. *J. Am. Chem. Soc.* **1987**, *109*, 769. (b) Chittipeddi, S.; Cromack, K. R.; Miller, J. S.; Epstein, A. J. *Phys. Rev. Lett.* **1987**, *22*, 2695.

(5) Candela, G. A.; Swartzendruber, L.; Miller, J. S.; Rice, M. J. *J. Am. Chem. Soc.* **1979**, *101*, 2755.

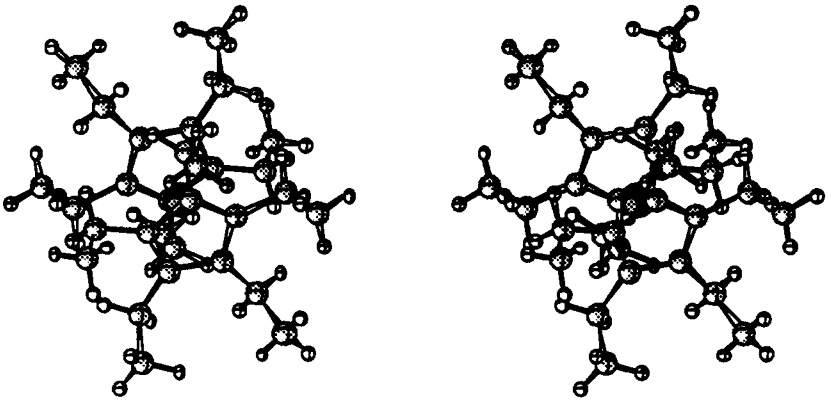

Figure 2. Stereoview of the cation $[Fe(C_5Et_5)_2]^{\bullet+}$.

X-ray Crystallographic Studies. The single-crystal structure of $[Fe(C_5Et_5)]_2^{\bullet+}[TCNQ]^{\bullet-}$ was solved by standard techniques using the Patterson heavy-atom method, which yielded the position of the Fe atom which lies on an inversion center. Hydrogen atoms were idealized and refined. The details of structural determination and fractional atomic coordinates are found in Tables I and II, and the atom labeling is presented in Figure 1. The remaining structural information is presented as supplementary material.

Results and Discussion

The 2,3,4,5-tetraethylcyclopent-2-enone (2) was synthesized by the literature method[6] with minor modification. C_5Et_5H (1) was prepared by the reaction of 2 with EtMgBr followed by acidic hydrolysis. The reaction of this with *n*-BuLi gave $Li(C_5Et_5)$. $Fe(C_5Et_5)_2$ was prepared from the reaction of $Li(C_5Et_5)$ and $FeCl_2$ in THF at 0 °C. Recrystallization from diethyl ether provided yellow prisms; $E_{1/2}° = -0.06$ V (CH_2Cl_2 or MeCN vs SCE $\{[NBu_4]^+[ClO_4]^-\}$).[7] Oxidation with $[Fe(C_5H_5)_2]^{\bullet+}[PF_6]^-$ leads to the isolation of $[Fe(C_5Et_5)_2]^{\bullet+}[PF_6]^-$. The 1:1 electron-transfer salts of $Fe(C_5Et_5)_2$ with TCNQ and TCNE were prepared from THF and MeCN, respectively. $[Fe(C_5Et_5)_2]^{\bullet+}[TCNE]^{\bullet-}$ is a green crystalline solid with $\nu_{C\equiv N}$ (Nujol) at 2182 and 2143 cm^{-1}. These absorptions are characteristic of $[TCNE]^n$ (n = 1−, and not n = 0 or 2−) or $[TCNE]_2^{-}$.[8,9] $[Fe(C_5Et_5)_2]^{\bullet+}[TCNQ]^{\bullet-}$ is a deep-blue solid with $\nu_{C\equiv N}$ (Nujol) at 2178 and 2152 cm^{-1}, which are characteristic of $[TCNQ]^n$ (n = 1−, but not n = 0 or 2−) or $[TCNQ]_2^{2-}$.[8,10]

Table II. Positional Parameters and Their Estimated Standard Deviations for $[Fe(C_5Et_5)_2][TCNQ]$

atom	x	y	z	B_{iso},[a] Å^2
Fe(1)	0	0	0	1.7 (1)′
N(1)	9156 (2)	6572 (2)	3442 (2)	4.9 (1)′
N(2)	5284 (2)	8279 (2)	2282 (2)	5.4 (1)′
C(1)	5765 (2)	5842 (2)	4286 (1)	3.3 (1)′
C(2)	6446 (2)	4938 (2)	4979 (2)	3.6 (1)′
C(3)	5702 (2)	4125 (2)	5663 (2)	3.6 (1)′
C(4)	6527 (2)	6674 (2)	3564 (1)	3.4 (1)′
C(5)	7976 (2)	6620 (2)	3493 (2)	3.7 (1)′
C(6)	5848 (2)	7574 (2)	2861 (2)	3.9 (1)′
C(10)	333 (2)	1958 (1)	1005 (1)	2.2 (1)′
C(11)	257 (2)	878 (1)	1760 (1)	2.2 (1)′
C(12)	1557 (2)	393 (1)	1851 (1)	2.1 (1)′
C(13)	2437 (1)	1172 (1)	1161 (1)	2.1 (1)′
C(14)	1676 (2)	2132 (1)	634 (1)	2.2 (1)′
C(15)	−767 (2)	2793 (2)	698 (2)	3.3 (1)′
C(15′)	−230 (3)	4108 (2)	1691 (2)	4.3 (1)′
C(16)	2220 (2)	3162 (2)	−154 (1)	3.1 (1)′
C(16′)	3289 (3)	4683 (2)	585 (2)	4.3 (1)′
C(17)	3935 (2)	1042 (2)	1051 (2)	3.0 (1)′
C(17′)	5466 (2)	2130 (3)	2043 (2)	4.7 (1)′
C(18)	1938 (2)	−728 (2)	2561 (1)	3.0 (1)′
C(18′)	3071 (3)	−93 (3)	3889 (2)	5.0 (1)′
C(19)	−967 (2)	345 (2)	2342 (1)	3.1 (1)′
C(19′)	−464 (3)	1178 (3)	3629 (2)	4.4 (1)′
H(2)	7413 (24)	4868 (20)	4980 (17)	4.0 (4)
H(3)	6254 (23)	3561 (21)	6134 (18)	4.3 (4)
H(15)	−1829 (23)	2176 (20)	548 (17)	3.8 (4)
H(15′)	−854 (26)	3078 (23)	−101 (22)	5.8 (5)
H(15′)	−1003 (26)	4600 (23)	1457 (20)	5.5 (5)
H(15′)	756 (31)	4730 (27)	1776 (22)	6.3 (6)
H(15″)	−126 (28)	3857 (25)	2456 (24)	6.3 (6)
H(16)	1300 (22)	3202 (18)	−775 (16)	3.3 (4)
H(16′)	2708 (23)	2777 (20)	−619 (18)	4.3 (4)
H(16′)	3678 (24)	5278 (22)	39 (20)	5.0 (5)
H(16′)	4163 (27)	4645 (22)	1131 (21)	4.9 (5)
H(16″)	2662 (31)	5056 (27)	984 (24)	7.0 (6)
H(17)	3951 (23)	1211 (21)	225 (19)	4.5 (4)
H(17′)	3861 (23)	56 (22)	1037 (18)	4.5 (4)
H(17′)	6362 (31)	1999 (25)	1981 (22)	6.3 (6)
H(17′)	5521 (32)	1985 (29)	2817 (29)	8.0 (8)
H(17″)	5550 (33)	3082 (34)	2009 (26)	8.5 (8)
H(18)	2345 (24)	−1322 (22)	2117 (18)	4.6 (4)
H(18′)	963 (23)	−1404 (20)	2557 (17)	4.0 (4)
H(18′)	3193 (30)	−896 (28)	4349 (23)	6.9 (6)
H(18′)	2792 (34)	608 (31)	4321 (27)	8.5 (8)
H(18″)	4096 (35)	441 (30)	3918 (25)	7.8 (8)
H(19)	−1187 (26)	−663 (25)	2379 (20)	5.6 (5)
H(19′)	−2017 (24)	313 (19)	1840 (17)	4.0 (4)
H(19′)	−1290 (27)	771 (24)	3945 (20)	5.7 (5)
H(19′)	−298 (30)	2157 (30)	3652 (23)	6.8 (6)
H(19″)	484 (30)	1085 (25)	4139 (22)	6.1 (6)

[a] The prime sign denotes four-thirds of the trace of the orthogonalized $\mathbf{B}_{ij}$ tensor.

Attempts to obtain the structure of the $[TCNE]^{\bullet-}$ salt was thwarted by the availability of only twinned crystals unsuitable for single crystal X-ray diffraction.[11] The structure for the $[TCNQ]^{\bullet-}$ salt was determined (Figure 1). The iron atom lies on an inversion center and the D_{5d} cation is ordered with the Fe–C, C–C, and C–Et bond distances ranging from 2.083 (1) to 2.111 (1), 1.430 (2) to 1.436 (2), and 1.497 (2) to 1.504 (2) Å (Table III) and average 2.095, 1.432, and 1.501 Å, respectively. Each C_5 ring is staggered with respect to each the other and the Fe–C_5 ring centroid is 1.705 Å. The values are comparable to those previously reported for $[FeCp^*_2]^{\bullet+}$.[4b] An unexpected structural feature is the conformation of the peripheral methyl groups which point away from the iron like a buttercup (Figure 2). The planar D_{2h} $[TCNQ]^{\bullet-}$ anion also lies on a point of symmetry and has average HC–CH,

---

(6) Best, W.; Fell, B.; Schmitt, G. *Chem. Ber.* **1976**, *109*, 2914.

(7) The reduction potential is within experimental error the same as observed for $FeCp_2^*$: Robins, J. L.; Edelstein, M.; Spenser, B.; Smart, J. C. *J. Am. Chem. Soc.* **1982**, *104*, 1882.

(8) Miller, J. S.; Dixon, D. A. *Science* **1987**, *235*, 871.

(9) Miller, J. S.; O'Hare, D. M.; Chackraborty, A.; Epstein, A. J. *J. Am. Chem. Soc.* **1989**, *111*, 7853.

(10) O'Hare, D. M.; Ward, M. D.; Miller, J. S. Submitted for publication.

(11) $[Fe(C_5Et_5)_2]^{\bullet+}[TCNE]^{\bullet-}$ was determined to have a tetragonal unit cell (a = 11.769 Å, c = 24.45 Å, V = 3387 Å^3).

Table III. Selected Bond Distances (Å) and Bond Angles (deg) for $[Fe(C_5Et_5)_2]^{•+}[TCNQ]^{•-}$

	Anion Bond Distances		
N(1)–C(5)	1.148 (2)	C(2)–C(3)	1.370 (2)
N(2)–C(6)	1.143 (2)	C(4)–C(5)	1.413 (3)
C(1)–C(2)	1.418 (2)	C(4)–C(6)	1.419 (3)
C(1)–C(3)^a	1.413 (3)	C(2)–H(2)	0.935 (19)
C(1)–C(4)	1.423 (2)	C(3)–H(3)	0.966 (20)
	Cation Bond Distances		
Fe(1)–C(10)	2.083 (1)	C(12)–C(13)	1.431 (2)
Fe(1)–C(11)	2.088 (1)	C(12)–C(18)	1.502 (2)
Fe(1)–C(12)	2.101 (1)	C(13)–C(14)	1.430 (2)
Fe(1)–C(13)	2.111 (1)	C(13)–C(17)	1.503 (2)
Fe(1)–C(14)	2.094 (1)	C(14)–C(16)	1.504 (2)
C(10)–C(11)	1.436 (2)	C(15)–C(15′)	1.516 (2)
C(10)–C(14)	1.431 (2)	C(16)–C(16′)	1.521 (2)
C(10)–C(15)	1.501 (2)	C(17)–C(17′)	1.520 (2)
C(11)–C(12)	1.432 (2)	C(18)–C(18′)	1.513 (2)
C(11)–C(19)	1.497 (2)	C(19)–C(19′)	1.514 (2)
	Anion Bond Angles		
N(1)-C(5)-C(4)	179.5 (3)	C(1)–C(2)–C(3)	121.1 (2)
N(2)–C(6)–C(4)	179.0 (3)	C(1)^a–C(3)–C(2)	121.5 (2)
C(2)–C(1)–C(3)^a	117.4 (1)	C(1)–C(4)–C(5)	121.5 (2)
C(2)–C(1)–C(4)	121.2 (2)	C(1)–C(4)–C(6)	121.6 (2)
C(3)^a–C(1)–C(4)	121.4 (2)	C(5)–C(4)–C(6)	116.9 (1)

^{a} $1 - x, 1 - y, 1 - z$.

HC–CC(CN)$_2$, ring–C(CN)$_2$, C–CN, and C≡N distances of 1.370, 1.416, 1.423, 1.416, and 1.146 Å, respectively (Table III). The NC–C–CN angle is 116.9°. These distances and angles are comparable to those previously reported.[12]

In the solid state the cation donors (D) and anion acceptors (A) form 1-D $\cdots D^{•+}A^{•-}D^{•+}A^{•-}\cdots$ chains analogous to the structures of $[FeCp^*_2]^{•+}[TCNQ]^{•-}$[12] and $[Fe(C_5Me_4H)_2]^{•+}[TCNQ]^{•-}$.[13] As cooperative ferromagnetic order is a bulk, not molecular, property, the intrachain as well as the interchain interactions are important in order to understand the spin–spin interactions which dominate the magnetic behavior. The chains are hexagonal closed-packed in the solid state with both in-registry and out-of-registry chains comparable to those reported for $[FeCp^*_2]^{•+}$[12] and $[Fe(C_5Me_4H)_2]^{•+}$[13] salts of $[TCNQ]^{•-}$. The unit cell has three unique interchain interactions, namely out-of-registry I and II and I and III, and in-registry I and IV (Figure 3). The in-registry intrachain separation is 8.84 Å and the out-of-registry intrachain separations are 9.28 and 9.38 Å. The former are 0.25 and 0.33 Å longer, and the latter, except for one comparable distances, are ≥0.7 Å longer than those reported for $[FeCp^*_2]^{•+}$[12] and $[Fe(C_5Me_4H)_2]^{•+}$[13] salts of $[TCNQ]^{•-}$.

The key inner- and intrachain Fe⋯Fe, Fe⋯N, and N⋯N separations are presented in Figure 3. The ferromagnetic 13.244-Å intrachain Fe⋯Fe spin-exchange distance[3] is substantially longer (2.70 and 2.86 Å, respectively) than those of the $[FeCp^*_2]^{•+}$[12] and $[Fe(C_5Me_4H)_2]^{•+}$[13] salts of $[TCNQ]^{•-}$ due to the steric requirements imposed by the additional methylene groups. The in-registry interchain Fe⋯Fe distance is 9.416 Å and is ~0.8 Å longer than those of the $[FeCp^*_2]^{•+}$[12] and $[Fe(C_5Me_4H)_2]^{•+}$[13] salts of $[TCNQ]^{•-}$. Likewise the out-of-registry interchain Fe⋯Fe distances (9.966, 11.257, 11.710, and 12.367 Å) are ~0.6 Å and ≥0.4 Å longer than those of the $[FeCp^*_2]^{•+}$[12] and $[Fe(C_5Me_4H)_2]^{•+}$[13] salts of $[TCNQ]^{•-}$, respectively. The ferromagnetic intrachain Fe⋯N spin-exchange distance[3] (Figure 3) due to the additional methylene groups are ≥1 Å longer for the $[Fe(C_5Et_5)_2]^{•+}$ salt. The shortest interchain Fe⋯N distance is 5.54 and is 0.3 Å longer than that observed for $[FeCp^*_2]^{•+}[TCNQ]^{•-}$[12] and is 0.75 Å longer than that observed for $[Fe(C_5Me_4H)_2]^{•+}[TCNQ]^{•-}$.[13] The antiferromagnetic N⋯N spin-exchange separation[3] of 5.16 Å is significantly longer (~1.2 Å) with respect to the $[FeCp^*_2]^{•+}$[12] and $[Fe(C_5Me_4H)_2]^{•+}$[13] salts of $[TCNQ]^{•-}$.

The ^{57}Fe Mössbauer spectra of the $[TCNE]^{•-}$ and $[TCNQ]^{•-}$ salts of $[Fe(C_5Et_5)_2]^{•+}$ differ significantly from the $[FeCp^*_2]^{•+}$ analogues with the $\cdots D^{•+}A^{•-}\cdots$ structural motif.[4b,12] The isomer shifts for $[Fe^{III}(C_5Et_5)_2]^{•+}$ (0.41 mm/s at room temperature) are typical of ferrocenium cations; however, differences lie in the low-temperature spectra. In contrast to $[FeCp^*_2]^{•+}[TCNE]^{•-}$, which exhibits fully resolved magnetic hyperfine splittings with internal fields of ~400 kG, arising from slow paramagnetic relaxation, extended cooperative 3-D order, or a complex combination of these effects,[4b] magnetic hyperfine splitting is not present for either $[Fe(C_5Et_5)_2]^{•+}[TCNE]^{•-}$ or $[Fe(C_5Et_5)_2]^{•+}[TCNQ]^{•-}$ at 1.5 K. This can be understood since $[Fe(C_5Et_5)_2]^{•+}$, with respect to $[FeCp^*_2]^{•+}$, has an effective lower symmetry, as detected by the sensitive Mössbauer spectra, which alters the single-ion orbital moment properties (e.g., anisotropy and magnitude) and interion interactions. This leads to dramatic consequences for hyperfine and magnetic exchange interactions. Consistent with the Mössbauer spectra, there is no evidence of either exchange interactions or incipient ordering in the susceptibility data for the $[TCNE]^{•-}$ and $[TCNQ]^{•-}$ salts (as reported for the $[Fe(C_5Me_4H)_2]^{•+}$[13] salts, which exhibit a dramatically reduced single-ion symmetry and fully resolved quadrupole interactions).

The magnetic susceptibility (2 – 320 K) was determined by the Faraday method[14] (Figure 4). The Curie–Weiss Θ values determined from the data taken above 80 K are 6.9, 7.5, and 6.1 K, and the effective moments μ_{eff} [$\equiv (8\chi T)^{1/2}$] are 3.37, 3.15, and 3.62 μ_B, respectively, for the $[PF_6]^-$, $[TCNE]^{•-}$, and $[TCNQ]^{•-}$ salts of $[Fe(C_5Et_5)_2]^{•+}$ above 30 K. The Θ values of +6.8 ± 0.7 K are suggestive of ferromagnetic interactions. The moments are much greater than expected from a randomly oriented sample based on $\langle g \rangle$ (i.e., 2.34 μ_B for $\langle g \rangle = 2.71$),[13] are less than expected for a sample oriented with the C_5 axis parallel to the magnetic field (i.e., 4.0 μ_B for $g_{\parallel} = 4.6$[15]), and are substantially greater than that expected for a sample oriented with the C_5 axis perpendicular to the magnetic field (i.e., 1.07 μ_B for $g_{\perp} = 1.24$). Thus, due to the orientation variability of polycrystalline samples of these salts (as suitably large single crystals are not available to measure the magnetic anisotropy), the observed effective moments are consistent either one or two $S = {}^1/_2$ radical(s) per formula unit contributing to the susceptibility with some field-induced orientation. Magnetic ordering, however, is not evident from the moment data (Figure 4), as a downturn in the moment is observed at below 10 K. Additionally, a field dependence in excess of that predicted by the Brillouin function is not observed.

Conclusion

On the basis of the infrared data, magnetic susceptibility, and available structural information, [Fe-

---

(12) Miller, J. S.; Reiff, W. M.; Zhang, J. H.; Preston, L. D.; Reis, A. H., Jr.; Gebert, E.; Extine, M.; Troup, J.; Dixon, D. A.; Epstein, A. J.; Ward, M. D. *J. Phys. Chem.* **1987**, *91*, 4344.

(13) Miller, J. S.; Glatzhofer, D. T.; O'Hare, D. M.; Reiff, W. M.; Chackraborty, A.; Epstein, A. J. *Inorg. Chem.* **1989**, *28*, 2930.

(14) Miller, J. S.; Dixon, D. A.; Calabrese, J. C.; Vazquez, C.; Krusic, P. J.; Ward, M. D.; Wasserman, E.; Harlow, R. L. *J. Am. Chem. Soc.* **1990**, *112*, 381.

(15) The 5-K EPR spectra of $[Fe(C_5Et_5)_2]^{•}1+$ as either the $[PF_6]^-$ or $[BF_4]^-$ salts in CH_2Cl_2 exhibit a strong absorption assignable to $g_{\parallel} = 4.59$. An absorption assignable to $g_{\perp} \sim 1.3$ typical of ferrocenium salts,[16] however, could not be clearly located.

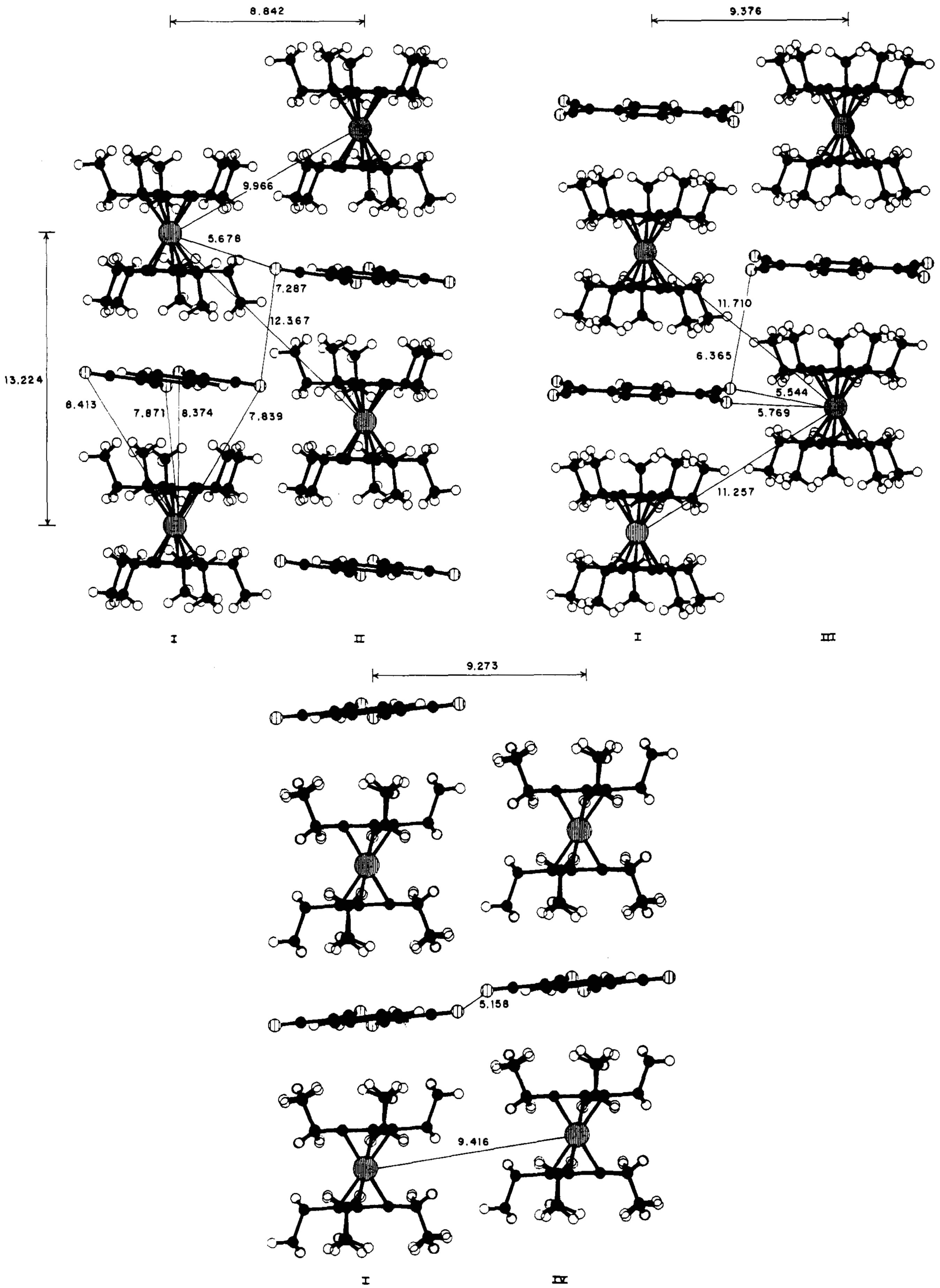

Figure 3. Out-of-registry interactions between chains I and II and I and III and in-registry interactions between chains I and IV.

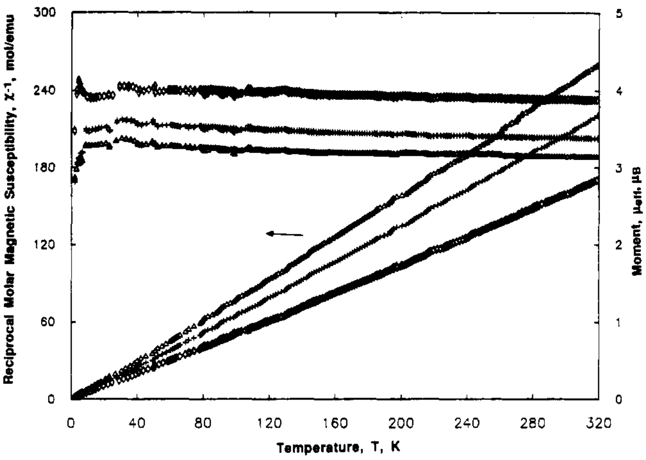

Figure 4. Reciprocal molar magnetic susceptibility, χ_M^{-1} (left), and moment, μ_{eff} (right), as a function of temperature for $[Fe(C_5Et_5)_2]^{\bullet+}[TCNE]^{\bullet-}$ (Δ), $[Fe(C_5Et_5)_2]^{\bullet+}[TCNQ]^{\bullet-}$ (◊), and $[Fe(C_5Et_5)_2]^{\bullet+}[PF_6]^{\bullet-}$ (+).

$(C_5Et_5)_2]^{\bullet+}[A]^{\bullet-}$ (A = TCNQ, TCNE) possesses isolated $S = {}^1/_2$ anions and a $\cdots D^{\bullet+}A^{\bullet-}D^{\bullet+}A^{\bullet-}\cdots$ structural motif analogous to the corresponding $[Fe(C_5Me_5)_2]^{\bullet+}$ salts.[3-5] The $[Fe(C_5Et_5)_2]^{\bullet+}$ salts exhibit ferromagnetic coupling as evidenced from Θ of +6.8 K. Ferromagnetic coupling has been previously attributed to interchain (1-D) interactions; however, due to the substantial increase in the intrachain Fe⋯Fe separation (2.70 Å), the coupling is expected to be significantly reduced. The interchain separations, albeit ≤0.33 Å longer, would appear to be the most important in determining the net magnetic coupling. Most significantly, the ferromagnetic Fe⋯N and the Fe⋯Fe separations are only slightly longer, while the interchain antiferromagnetic N⋯N interactions are substantially longer (~1.2 Å) suggesting that ferromagnetic coupling would dominate. Unlike the $[Fe(C_5Me_5)_2]^{\bullet+}$ salts, however, the $[Fe(C_5Et_5)_2]^{\bullet+}$ salts do not exhibit magnetic ordering and a field dependence of the magnetization characteristic of long-range (bulk) magnetic ordering. Thus, the inter- and intrachain spin separations are longer, and this leads to weaker exchange interactions and a critical temperature reduced below 1.5 K.

Acknowledgment. K.-M.C. and J.S.M. gratefully acknowledge partial support by the U.S. Department of Energy, Division of Materials Science (Grant No. DE-FG02-86ER45271.A000). We also appreciate the synthetic assistance provided by C. Vazquez, the electrochemical data taken by E. Delawski and M. D. Ward, the crystallographic expertise supplied by W. Marshall, ERP spectra by F. W. Barney and P. J. Krusic, and the Faraday susceptibility data taken by R. S. McLean (Du Pont CR&DD) as well as insightful discussions with A. J. Epstein (The Ohio State University).

Supplementary Material Available: For $[Fe(C_5Et_5)_2]^{\bullet+}[TCNQ]^{\bullet-}$ tables of anisotropic thermal parameters, bond distances, bond angles, and intermolecular separations (5 pages); a listing of observed and calculated structure factors (12 pages). Ordering information is given on any current masthead page.

Isocyanide Ligands in Tp′(CO)$_2$IMo(CNR) Complexes as Precursors to Aminocarbyne, η^2-Iminoacyl, and η^2-Vinyl Ligands

A. S. Gamble, P. S. White, and J. L. Templeton*

Department of Chemistry, University of North Carolina, Chapel Hill, North Carolina 27599

Received August 30, 1990

A mixture of molybdenum aminocarbyne, η^2-iminoacyl, and η^2-acyl complexes, $Tp'(CO)_2Mo{\equiv}CN(Me)(Bu^t)$, $Tp'(CO)_2Mo(\eta^2\text{-}C(NBu^t)Me)$, and $Tp'(CO)(Bu^tNC)Mo(\eta^2\text{-}C(O)Me)$, has been prepared via the addition of MeI to the anionic *tert*-butyl isocyanide complex $[Na][Tp'(CO)_2Mo(CNBu^t)]$. Addition of MeI to the analogous anionic methyl or phenyl isocyanide complex yields only aminocarbyne complexes. The η^2-iminoacyl complex can be deprotonated at the C_β methyl site with KH to give an anionic η^2-enamide intermediate, and quenching with MeI yields the ethyl product, $Tp'(CO)_2Mo(\eta^2\text{-}C(NBu^t)Et)$. The η^2-iminoacyl complex undergoes cleavage in air to give *N*-*tert*-butylacetamide. Protonation of $Tp'(CO)_2Mo{\equiv}CN(Me)(Bu^t)$ in the presence of phenylacetylene ultimately yields a cationic η^2-vinyliminium complex, $[Tp'(CO)_2Mo(\eta^2\text{-}C(Ph){=}C(H)C(H){=}N(Me)(Bu^t))][BF_4]$. This material is fluxional in the ^1H NMR spectrum due to rapid inversion at the vinyl β-carbon. The X-ray structure of this η^2-vinyl cation is reported. A neutral η^2-vinylamine complex, $Tp'(CO)_2Mo(\eta^2\text{-}C(Ph){=}C(H)CH_2N(Me)(Bu^t))$, has been synthesized by addition of $LiEt_3BH$ to the cationic η^2-vinyliminium complex.

Introduction

The chemistry of transition-metal isocyanide complexes complements the chemistry of metal carbonyl complexes.[1] Two modes of reactivity dominate electrophilic addition to metal isocyanides. First, isocyanide complexes, like carbonyl complexes,[2] undergo migratory insertion with alkyl ligands.[3] A common synthetic route to η^2-iminoacyl

---

(1) Singleton, E.; Oosthuizen, H. E. *Adv. Organomet. Chem.* **1983**, *22*, 209.

(2) (a) Fachinetti, G.; Floriani, C. *J. Organomet. Chem.* **1974**, *71*, C5. (b) Fachinetti, G.; Fochi, G.; Floriani, C. *J. Chem. Soc., Dalton Trans.* 1977, 1946. (c) Marsella, J. A.; Moloy, K. G.; Caulton, K. G. *J. Organomet. Chem.* **1980**, *201*, 389. (d) Curtis, M. D.; Shiu, K.-B.; Butler, W. M. *J. Am. Chem. Soc.* **1986**, *108*, 1550.

0276-7333/91/2310-0693$02.50/0